Estimating the altitude of volcanic sulfur dioxide plumes from space borne hyper-spectral UV measurements

Kai Yang,[1,2] Xiong Liu,[1,2] Nickolay A. Krotkov,[1,2] Arlin J. Krueger,[3] and Simon A. Carn[4]

Received 5 March 2009; revised 14 April 2009; accepted 17 April 2009; published 19 May 2009.

[1] The altitude of volcanic sulfur dioxide (SO_2) plumes determines the transport and atmospheric residence time of derived sulfate aerosol, and hence their impacts on the environment and climate. Knowledge of the altitude of fresh eruption clouds is also very important in aviation safety to avoid flying through ash clouds and for forecasting of plume drift. In this paper, we demonstrate the altitude dependence of the spectral response in the backscattered ultraviolet (BUV) radiance when a SO_2 absorption layer is added to an ozone-laden atmosphere. The distinctive spectral response serves as the physical basis for simultaneous SO_2 loading and altitude retrievals, which can improve the characterization of volcanic emissions. We accomplish this by extending the recently developed Iterative Spectral Fitting (ISF) algorithm to include effective plume altitude determination when performing simultaneous ozone and SO_2 retrievals. The extended ISF algorithm is applied to hyper-spectral Ozone Monitoring Instrument (OMI) measurements of two volcanic eruptions: Sierra Negra in October 2005 and Jebel al Tair in September 2007. The results show for the first time that a wide range of SO_2 plume altitudes can be estimated directly from hyper-spectral BUV radiance measurements. **Citation:** Yang, K., X. Liu, N. A. Krotkov, A. J. Krueger, and S. A. Carn (2009), Estimating the altitude of volcanic sulfur dioxide plumes from space borne hyper-spectral UV measurements, *Geophys. Res. Lett.*, *36*, L10803, doi:10.1029/2009GL038025.

1. Introduction

[2] Volcanic emissions are a major natural source of sulfur dioxide (SO_2) and other trace gases, perturbing atmospheric composition and chemistry, and hence potentially affecting the environment and climate. These effects are primarily due to the conversion of volcanic sulfur-containing gases (mostly SO_2 and minor amounts of H_2S) to sulfate aerosols [*Robock*, 2000]. These volcanic impacts are exemplified by the June 1991 Pinatubo (Philippines) eruption, which injected a large amount of SO_2 (~20 Megatons) [*Bluth et al.*, 1992] and ash directly into the stratosphere, up to 35 km above sea level (ASL). While the ash from this eruption fell out of the atmosphere in days, the sulfate aerosol derived from the SO_2 persisted in the stratosphere for years, lowered the global surface temperature on average by 0.5°C [*McCormick et al.*, 1995] and produced record lows in global ozone in 1992 [*Gleason et al.*, 1993]. This eruption also illustrates the hazard to aircraft posed by volcanic ash.

[3] In general the impacts of volcanic emissions increase with the atmospheric loading and residence time of the resulting sulfate aerosol. While the aerosol loading is proportional to the amount of sulfur-containing gases in the volcanic plume, the aerosol residence time is highly dependent on the plume altitude, at which the sulfur-containing gases oxidize to sulfuric acid (H_2SO_4) that condenses into sulfate aerosol. To evaluate the impacts of volcanic emissions, it is important not only to quantify SO_2 abundances but also to determine SO_2 injection altitude.

[4] Nadir-viewing satellite sensors, beginning with the Total Ozone Mapping Spectrometer (TOMS) [*Krueger et al.*, 1995] and followed by other ultraviolet (UV) and infrared (IR) instruments, have long been employed to monitor volcanic SO_2 emissions with variable sensitivity and coverage. Until recently all SO_2 retrieval algorithms make explicit or implicit assumptions about the SO_2 vertical distribution in deriving total columns from these nadir radiances, resulting in errors in the retrieved results when the assumptions are not valid. Recently, two new techniques have been developed to estimate the altitude of SO_2 in a volcanic eruption cloud. One is based on the optimal estimation technique applied to hyper-spectral IR measurements that include the SO_2 absorption band centered at 7.34 μm from the Infrared Atmospheric Sounding Interferometer (IASI) [*Clarisse et al.*, 2008], and the other is based on inverse trajectory modeling that assigns appropriate SO_2 amounts at different altitudes in order to minimize the difference between satellite SO_2 column maps and those derived from the trajectory model [*Eckhardt et al.*, 2008]. Both techniques have demonstrated their potential using the September 2007 eruption of Jebel al Tair (Yemen). Satellite BUV measurements in the 305–330 nm wavelength range provide the most sensitive detection of SO_2 in the atmosphere, however to date there has been no attempt to obtain vertical information about SO_2 plumes (volcanic or otherwise) directly from these measurements, even though they have been used to retrieve vertical profiles of ozone [*Bhartia et al.*, 1996; *Liu et al.*, 2005a]. The averaging kernels of the Linear Fit (LF) algorithm show that SO_2 retrievals have significant dependence on the plume altitude [*Yang et al.*, 2007], hinting that this dependence may be exploited for SO_2 plume altitude estimation.

[5] In this paper, we describe the sensitivity of BUV measurements to the altitude at which a SO_2 layer is introduced into the atmosphere, and extend the Iterative

[1]GEST, University of Maryland Baltimore County, Baltimore, Maryland, USA.
[2]Laboratory of Atmospheres, NASA Goddard Space Flight Center, Greenbelt, Maryland, USA.
[3]JCET, University of Maryland Baltimore County, Baltimore, Maryland, USA.
[4]Department of Geological and Mining Engineering and Sciences, Michigan Technological University, Houghton, Michigan, USA.

0094-8276/09/2009GL038025$05.00

Spectral Fitting (ISF) algorithm [*Yang et al.*, 2009] to perform simultaneous retrievals of ozone column, SO_2 column, and effective SO_2 altitude. This extended ISF algorithm is applied to volcanic plumes from two recent eruptions.

2. Ozone Monitoring Instrument

[6] Flying on NASA's Aura spacecraft since July 2004, the Dutch-Finnish built Ozone Monitoring Instrument (OMI) [*Levelt et al.*, 2006] is a nadir-viewing hyper-spectral imaging spectrometer designed to measure both the back-scattered radiance from Earth and the incoming solar irradiance using UV and visible (VIS) channels (full performance ranges 270–365 nm and 366–500 nm, respectively). The Hartley-Huggins bands of ozone and the SO_2 absorption band are located and overlap in the range of the UV channel, which is optically separated into UV-1 (270–310 nm) and UV-2 (310–365 nm) sub-channels to reduce stray light below 310 nm. The UV-2 channel has a spectral resolution of ~0.42 nm, a spectral sampling rate of 0.15 nm/pixel and a spatial resolution of 13 × 24 km^2 at nadir; UV-1 has a spectral resolution of ~0.63 nm, a spectral sampling rate of 0.32 nm/pixel and a nadir spatial resolution of 13 × 48 km^2. Essentially the sampling and resolution of UV-1 are equivalent to co-adding four UV-2 pixels, two each in the spectral and spatial (cross-track) dimensions. By combining hyper-spectral capability with its relatively small footprint size and daily global coverage, OMI is providing unique data for improving our understanding of atmospheric composition and chemistry.

3. SO_2 Plume Altitude Estimation

[7] When a thin SO_2 layer is introduced into the atmosphere, its altitude determines the proportion of back-scattered photons that pass through this absorbing layer after the last scattering toward the sensor. Clearly, the lower the layer in the atmosphere, the more photons are Rayleigh backscattered in the overlying atmosphere, resulting in fewer photons transmitted through the layer, and vice versa. As a result, BUV radiance measurements (e.g., in the OMI UV channel) contain quantitative information about the layer altitude, in addition to information about atmospheric constituents. For an infinitesimal SO_2 layer (i.e., both the thickness and column amount, Ξ, approach zero) at an altitude z, the top-of-atmosphere (TOA) BUV radiance at a wavelength (λ) can be expressed analytically as $I_{z,\lambda}(\Xi) = I_\lambda(0)\exp(-A_{z,\lambda}\alpha_{z,\lambda}\Xi)$ (a similar equation is used as the basis for the DOAS method [*Platt*, 1994]) according to the Beer-Lambert law, where $I_\lambda(0)$ is the TOA BUV radiance for the SO_2 free atmosphere, $\alpha_{z,\lambda}$ is the temperature dependent SO_2 absorption coefficient [$\frac{1}{atm-cm}$] [see *Yang et al.*, 2007, Figure 1], and $A_{z,\lambda}$ is the ratio of average photon path length (at z) over the layer geometric thickness (this ratio is also called the altitude dependent air mass factor) [*Liu et al.*, 2005b; *Eskes and Boersma*, 2003] for photons contributing to the TOA BUV radiance. The subscript λ will be dropped from subsequent notation in this paper.

[8] To illustrate the relative TOA radiance change induced by the changes in a SO_2 layer, we derive the corresponding weighting functions (WF), which can be analytically expressed (for the infinitesimal SO_2 layer considered above) as $k_\Xi = \frac{\partial \ln I_z}{\partial \Xi} = -\alpha_z A_z$ and $k_z = \frac{\partial \ln I_z}{\partial z} = (-\alpha_z \frac{\partial A_z}{\partial z} - A_z \frac{\partial \alpha_z}{\partial z})\Xi$, respectively for the layer column Ξ and layer altitude z. We show the air mass factor A_z (Figure 1a, divided by geometric air mass factor A_g), its vertical gradient $\frac{\partial A_z}{\partial z}$ (Figure 1b, also normalized by A_g), the layer column WF k_Ξ (Figure 1c), and the layer altitude WF k_z (Figure 1d, normalized by the layer column Ξ). A perturbation in the SO_2 layer, either in layer column amount or layer altitude, changes the SO_2 absorption experienced by the BUV photons, as both WFs contain the term of SO_2 absorption coefficient. Therefore both Figures 1c and 1d show the high frequency band structure of the SO_2 cross-section (in other words, these two WFs are correlated). However, different physical mechanisms are responsible for the absorption change induced by the different perturbations: a change in layer amount Ξ causes a direct change in the layer absorption optical thickness, so k_Ξ is proportional to the local air mass factor A_z, while a change in layer altitude z induces both a direct change in the number of photons passing through the layer and an indirect change in the layer absorption optical thickness due to the temperature variation with altitude. Since the SO_2 cross-section is only weakly temperature dependent, the WF k_z is usually dominated by its first term, $-\alpha_z \Xi \frac{\partial A_z}{\partial z}$, which shows that radiance change (in log space) induced by the altitude perturbation is proportional to the vertical gradient of A_z. The correlation between the layer column and altitude WFs mentioned above implies that an error in layer altitude z can induce an error in layer column Ξ, and vice versa. However the distinctive wavelength and altitude dependence patterns in Figures 1a and 1b indicate that changes in SO_2 amount cause different spectral responses in the BUV radiances to those caused by changes in layer altitude. Therefore BUV radiance measurements can be used to extract these two quantities. Note that the layer altitude WF (Figure 1c) for an unit SO_2 layer is much smaller than the corresponding layer column WF (Figure 1d). However the magnitude of the altitude spectral response increases with larger absorption optical thickness of the plume, hence its altitude may be accurately extracted only when there is a significant amount of SO_2. The layer column and altitude WFs defined for SO_2 also apply to other trace gases, such as BrO, NO_2, and HCHO, with α_z replaced by the corresponding absorption coefficients. But it is usually difficult to estimate the altitudes of these trace gases due to the small absorption optical thickness in the range 300–330 nm associated with their typically low loadings.

[9] For lower tropospheric SO_2 layers, BUV measurements at wavelengths longer than 310 nm (e.g., in the OMI UV-2 channel) can discriminate altitude because the SO_2 altitude sensitivity is strong in the troposphere (<10 km) and peaks in the lower troposphere and boundary layer (see Figures 1b and 1c). To resolve higher altitude (>10 km) SO_2 layers, BUV measurements at shorter wavelengths (<310 nm; e.g., in the OMI UV-1 channel) are required. At wavelengths shorter than 300 nm, there is very little column or altitude sensitivity to typical volcanic SO_2 clouds (<25 km altitude), although if a volcanic plume reaches very high altitudes (>25 km), measurements at these wavelengths can be used to detect its altitude.

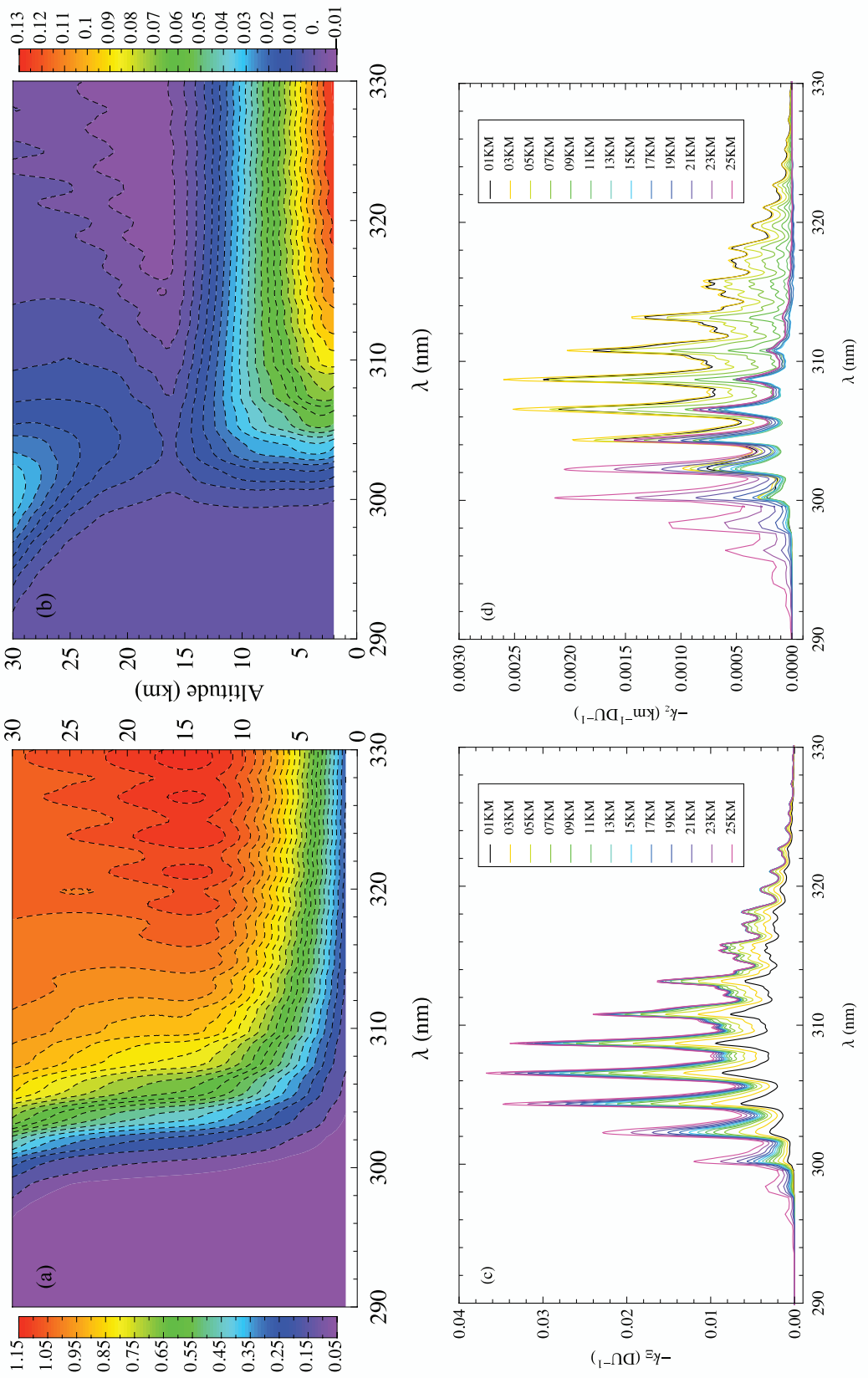

Figure 1. (a) Air mass factor, (b) its vertical gradient, (c) the SO_2 column, and (d) altitude weighting functions are computed for a typical observing condition: climatological midlatitude ozone profile with total column 325 DU under a clear sky, with a surface albedo 0.05, nadir viewing with a solar zenith angle 45°. Note that the air mass factor (Figure 1a) and its vertical gradient (Figure 1b) are normalized by the geometrical air mass factor.

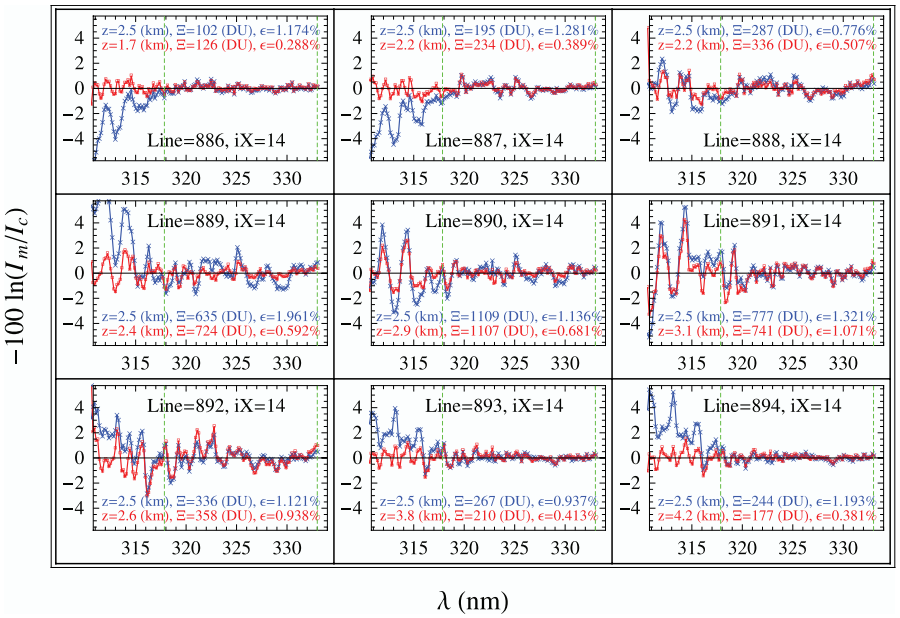

Figure 2. Fitting residuals, computed as the difference (in log space) between the sun-normalized measured radiance (I_m) and the calculated radiance (I_c), for assumed plume altitude (blue) and estimated plume altitude (red), are shown for a few pixels. Retrieved SO_2 columns (Ξ) and fitting errors (ϵ) are listed next to the corresponding plume altitudes (z) used in the ISF retrievals. The blue curves are for ISF retrievals with assumed central altitude at 2.5 km with 3.5 km plume width (defined as the full width at half maximum of the Gaussian profile), while the red curves correspond to altitudes estimated from iterative adjustment starting at 2.5 km altitude with 2.4 km plume width.

[10] We have extended the ISF algorithm, which performs simultaneous ozone and SO_2 column retrievals [*Yang et al.*, 2009], to include SO_2 plume altitude estimation. The extended algorithm derives the SO_2 altitude by adjusting it in successive ISF retrievals until the residuals, i.e., differences between measurements and forward model computations, are minimized, since a difference between the assumed and the actual SO_2 altitudes produces residuals that can not be well compensated in the 300–330 nm range by adjusting the SO_2 column alone. Note that higher SO_2 amounts will change the air mass factor shown in Figure 1a, and can further increase the altitude sensitivity. Without using the analytic equations of the TOA radiance and the corresponding WFs derived for an infinitesimal SO_2 layer, the extended ISF algorithm employs accurate radiative transfer calculation of the TOA radiance for any given ozone and SO_2 columns with the corresponding a priori profiles. Doing so properly accounts for the nonlinear effect by updating the linearization point and WFs at each iteration [*Yang et al.*, 2009].

[11] The vertical distribution of a volcanic SO_2 plume is very different from the typical broad ozone profile and is usually narrowly confined due to its transient source of emission and its dispersion by wind shear. It is not possible to resolve the precise profile of a volcanic plume using BUV measurements, which provide a vertical resolution of about 5–8 km in the stratosphere and about 10 km in the troposphere [*Bhartia et al.*, 1996; *Liu et al.*, 2005a]. Therefore we represent the SO_2 plume using a Gaussian profile, characterized by a central altitude and width. The central altitude of the Gaussian derived from the extended ISF retrievals should represent the effective altitude, equivalent to the altitude at the center of SO_2 mass when the layer is thin.The precision of the derived effective altitude is higher than the profile vertical resolutions due to the reduction in retrieval dimension. For example, given a 10 Dobson Unit (1 DU = 0.001 atm-cm = 2.69×10^{16} molecules/cm^2) SO_2 plume and the OMI UV-2 signal-to-noise ratio of ~1000 [*Levelt et al.*, 2006], the estimated precision of the effective altitude is ~0.1 km when the plume is located in the troposphere.

4. Case Studies

[12] We have applied the extended ISF algorithm described above to OMI observations of volcanic plumes from two eruptions, the Sierra Negra eruption (Galàpagos Islands, Ecuador) in October 2005 and the Jebel al Tair eruption (Yemen) in September 2007. These cases were selected because the altitudes of these plumes span a range from the lower troposphere to the stratosphere.

4.1. Sierra Negra Eruption in October 2005

[13] The Sierra Negra plume resulted from an effusive eruption, characterized by sustained strong gas emissions into the lower troposphere. In a previous paper, we applied the ISF technique to this plume to demonstrate greatly improved quantification of large SO_2 columns through proper treatment of non-linear SO_2 absorption effects [*Yang et al.*, 2009]. The ISF retrievals can be further improved by simultaneous determination of effective SO_2 plume altitude, which can be achieved using the OMI UV-2 measurements alone for this lower tropospheric plume. In Figure 2, we compare the ISF fitting residuals from retrievals with fixed (assumed) and retrieved SO_2 plume altitudes for a few pixels along the orbital track for the OMI cross-track

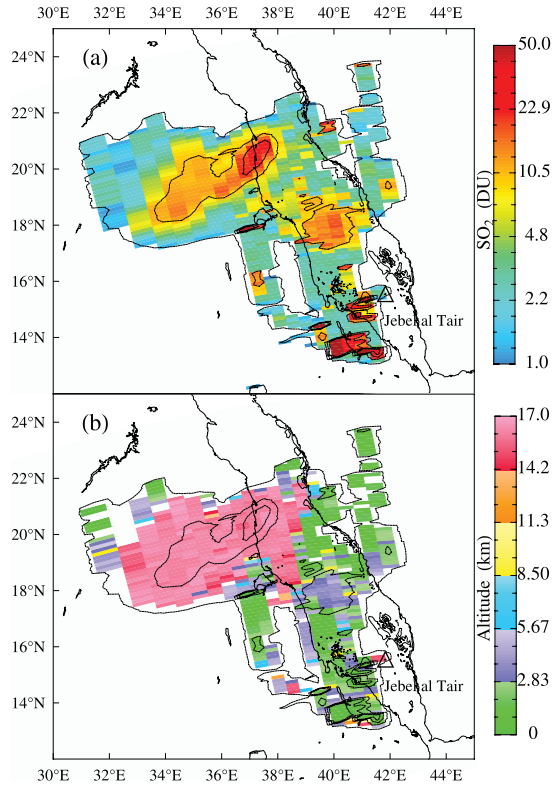

Figure 3. (a) SO_2 vertical column and (b) effective altitude maps derived from OMI UV (both UV-1 and UV-2) radiances for the Jebel al Tair volcanic plume at 10:59 UT on October 1, 2007, using the extended ISF algorithm.

position that covers the vent of the volcano (where the largest SO_2 column was measured [*Yang et al.*, 2009]). It is clear that higher precision retrievals, as indicated by much smaller fitting errors (ϵ) computed as the standard deviation of the residuals in the 310.8–333 nm range, are achieved by adjusting the plume central altitude. The smaller fitting errors are mostly a result of better fitting at short wavelengths, though noticeably smaller residuals in the ozone and SO_2 fitting window (delimited by the two dashed green lines of Figure 2) also contribute to the reduction in fitting error. The effective plume altitudes determined from the retrievals show that the plume rose gradually along the ascending orbital track from 1.7 km to 4.2 km altitude in a distance slightly over 100 km. These altitudes are consistent with near simultaneous IR observations from the Atmospheric Infrared Sounder (AIRS; on the Aqua satellite in the A-Train), which did not detect any significant SO_2 in the same region, indicating that it was located below 5 km altitude where water vapor absorption overwhelms the SO_2 absorption [*Carn et al.*, 2005].

4.2. Jebel al Tair Eruption in September 2007

[14] Jebel al Tair volcano (Yemen) erupted unexpectedly on September 30, 2007 after that afternoon's OMI overpass, injecting gases high into the atmosphere. When OMI made its first observation of this event on October 1, 2007, the plume from the initial explosive eruption had drifted away from the volcano, which continued to erupt effusively and release gases into the lower troposphere. The extended ISF retrievals, depicted as column and altitude maps in Figure 3, reveal a large part of the plume located northeast of Jebel al Tair at about 16 km ASL. Closer to the volcano, the effusive plume is also northeast of the volcano but at altitudes of around 4 km ASL. Note that in this case both OMI UV-1 and UV-2 measurements are used in the extended ISF retrievals. Without the short wavelength measurements (<310 nm, OMI UV-1), it would not be possible to resolve the altitude once the plume reaches the upper troposphere (>10 km), where the longer wavelength measurements (OMI UV-2) have minimal altitude sensitivity (Figure 1b).

[15] The 16 km plume altitude is near the local tropopause altitude of 15.3 km [*Eckhardt et al.*, 2008], indicating that the explosive eruption injected SO_2 into the upper troposphere and lower stratosphere (UTLS), consistent with the IR (IASI) observations and inverse transport modeling. IR sensors (AIRS, IASI) also detected the lower part of the plume northwest of Jebel al Tair, but were unable to detect any SO_2 at low altitudes immediately surrounding the volcano, and also missed the part of the plume to the southwest (see figures by *Eckhardt et al.* [2008] and *Clarisse et al.* [2008]). In contrast, OMI observed significantly elevated SO_2 loadings at altitudes below 3 km in the latter regions, most likely sourced from sustained emissions from the ongoing effusive eruption.

5. Summary

[16] We have elucidated the different physical mechanisms through which the column content and altitude of a volcanic SO_2 plume affects BUV radiances, and showed that BUV radiances in different spectral ranges exhibit different sensitivities to plumes at different altitudes. Based on these findings, we have extended the ISF algorithm to simultaneously retrieve the SO_2 column amount in a volcanic plume and its effective altitude from BUV radiance measurements. Applications of this extended ISF algorithm to OMI observations of recent volcanic eruptions demonstrate for the first time that SO_2 plume altitudes can be derived directly from satellite BUV measurements. The retrieved SO_2 altitudes can distinguish between a plume in the lower troposphere, upper troposphere, or stratosphere, which is crucial for aviation hazard mitigation. The applications of the extended ISF algorithm also show decreased SO_2 column errors because the uncertainties in SO_2 retrievals introduced by assumed plume altitudes are reduced.

[17] Future work will investigate the impact of inhomogeneity in the OMI field of view on the retrieved SO_2 column and altitude, as this has likely suppressed the retrieved altitudes for some pixels on and near the edge of the plume as shown in Figure 3b. We will also investigate the impact of aerosols, especially volcanic ash, on the plume altitude estimation.

[18] **Acknowledgments.** This work was supported in part by NASA under grant NNS06AA05G (NASA volcanic cloud data for aviation hazards).

References

Bhartia, P. K., R. D. McPeters, C. L. Mateer, L. E. Flynn, and C. Wellemeyer (1996), Algorithm for the estimation of vertical ozone profiles from the backscattered ultraviolet technique, *J. Geophys. Res.*, *101*, 18,793–18,806.

Bluth, G. J. S., S. D. Doiron, C. C. Schnetzler, A. J. Krueger, and L. S. Walter (1992), Global tracking of the SO_2 clouds from the June, 1991 Mount Pinatubo eruptions, *Geophys. Res. Lett.*, *19*, 151–154.

Clarisse, L., P. F. Coheur, A. J. Prata, D. Hurtmans, A. Razavi, T. Phulpin, J. Hadji-Lazaro, and C. Clerbaux (2008), Tracking and quantifying volcanic SO_2 with IASI, the September 2007 eruption at Jebel at Tair, *Atmos. Chem. Phys.*, *8*, 7723–7734.

Carn, S. A., L. L. Strow, S. de Souza-Machado, Y. Edmonds, and S. Hannon (2005), Quantifying tropospheric volcanic emissions with AIRS: The 2002 eruption of Mt. Etna (Italy), *Geophys. Res. Lett.*, *32*, L02301, doi:10.1029/2004GL021034.

Eckhardt, S., A. J. Prata, P. Seibert, K. Stebel, and A. Stohl (2008), Estimation of the vertical profile of sulfur dioxide injection into the atmosphere by a volcanic eruption using satellite column measurements and inverse transport modeling, *Atmos. Chem. Phys.*, *8*, 3881–3897.

Gleason, J., et al. (1993), Record low global ozone in 1992, *Science*, *260*, 523–525.

Eskes, H. J., and K. F. Boersma (2003), Averaging kernels for DOAS total-column satellite retrievals, *Atmos. Chem. Phys.*, *3*, 1285–1291.

Krueger, A. J., L. S. Walter, P. K. Bhartia, C. C. Schnetzler, N. A. Krotkov, I. Sprod, and G. J. S. Bluth (1995), Volcanic sulfur dioxide measurements from the total ozone mapping spectrometer instruments, *J. Geophys. Res.*, *100*, 14,057–14,076.

Levelt, P. F., G. H. J. van den Oord, M. R. Dobber, A. Mälkki, H. Visser, J. de Vries, P. Stammes, J. Lundell, and H. Saari (2006), The Ozone Monitoring Instrument, *IEEE Trans. Geosci. Remote Sens.*, *44*, 1093–1101, doi:10.1109/TGRS.2006.872333.

Liu, X., K. Chance, C. E. Sioris, R. J. D. Spurr, T. P. Kurosu, R. V. Martin, and M. J. Newchurch (2005a), Ozone profile and tropospheric ozone retrievals from the Global Ozone Monitoring Experiment: Algorithm description and validation, *J. Geophys. Res.*, *110*, D20307, doi:10.1029/2005JD006240.

Liu, X., C. E. Sioris, K. V. Chance, T. P. Kurosu, M. J. Newchurch, R. V. Martin, and P. I. Palmer (2005b), Mapping tropospheric ozone profiles from an airborne UV/Visible spectrometer, *Appl. Opt.*, *44*, 3312–3319.

McCormick, M. P., L. W. Thomason, and C. R. Trepte (1995), Atmospheric effects of the Mt. Pinatubo eruption, *Nature*, *373*, 399–404, doi:10.1038/373399a0.

Platt, U. (1994), Differential optical absorption spectroscopy (DOAS), in *Air Monitoring by Spectroscopic Techniques*, *Chem. Anal. Ser.*, vol. 127, edited by M. Siegrist, pp. 27–84, John Wiley, New York.

Robock, A. (2000), Volcanic eruption and climate, *Rev. Geophys.*, *38*, 191–219.

Yang, K., N. A. Krotkov, A. J. Krueger, S. A. Carn, P. K. Bhartia, and P. F. Levelt (2007), Retrieval of large volcanic SO_2 columns from the Aura Ozone Monitoring Instrument: Comparison and limitations, *J. Geophys. Res.*, *112*, D24S43, doi:10.1029/2007JD008825.

Yang, K., N. A. Krotkov, A. J. Krueger, S. A. Carn, P. K. Bhartia, and P. F. Levelt (2009), Improving retrieval of volcanic sulfur dioxide from backscattered UV satellite observations, *Geophys. Res. Lett.*, *36*, L03102, doi:10.1029/2008GL036036.

S. A. Carn, Department of Geological and Mining Engineering and Sciences, Michigan Technological University, Houghton, MI 49931, USA.

N. A. Krotkov, X. Liu, and K. Yang, NASA Goddard Space Flight Center, Mail Code 613.3, Greenbelt, MD 20771–0001, USA. (kai.yang-1@nasa.gov)

A. J. Krueger, JCET, University of Maryland Baltimore County, Baltimore, MD 21250, USA.